Global NEST Journal, Vol 25, No 2, pp 67-74

The synthesis of titania nanoparticles (TiO_2) and its methylene blue dye removal efficiency through photocatalysis based on response surface methodology (RSM)

Kanwal H.[1*], Tahir H.[2], Shah A.R.[2], Ahmed W.[1], and Arsalan M.[3]
[1]Institute of Environmental Studies, University of Karachi, Karachi City, 75270, Pakistan
[2]Department of Chemistry, University of Karachi, Karachi City, 75270, Pakistan
[3]Department of Geology, University of Karachi, Karachi City, 75270, Pakistan
Received: 31/05/2022, Accepted: 13/01/2023, Available online: 26/01/2023
*to whom all correspondence should be addressed: e-mail: humairakanwal@uok.edu.pk
https://doi.org/10.30955/gnj.004359

Graphical abstract

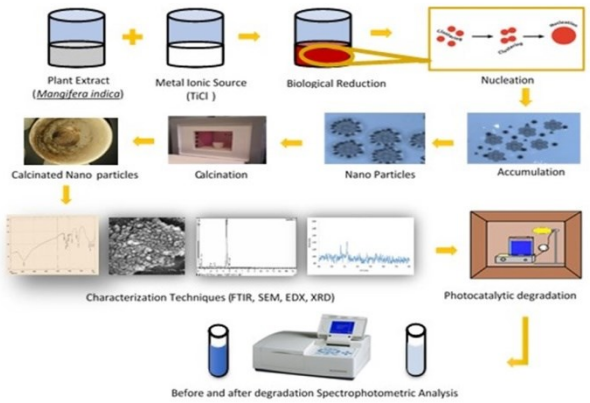

Abstract

Water pollution has been acknowledged as an issue of concern due to recalcitrant pollutants like textile dyes. Therefore, the eco-friendly synthesis of nano-particles (NPs) through green chemistry approach from sources and materials of organic origin has not only enhanced the properties of substance at nanoscale but has also reduced the toxicological impacts on human health and environment. In this study a successful attempt was made to synthesize TiO_2 NPs by *Mangifera indica* leaves extract as organic source. The structural morphology was determined by carrying out FTIR, SEM, EDX and XRD techniques. The removal of Methylene Blue (MB) dye was assessed by the application of photocatalysis technique. The experiments were designed using RSM (CCD) approach for selected parameters such as pH, TiO_2 NPs, Dye concentration and Time. The maximal dye removal efficiency of 98% was achieved at optimum conditions of 4.7 pH, 0.04g of nano photocatalyst in 250ml of dye solution having 8ppm concentration, allowed to react for 45 min. The regression coefficient value of 79.37% was determined by ANOVA for MB dye. The results clearly indicate that the application of green nanoparticles for the removal of MB dye is a feasible option to overcome with the ever-increasing issue of water pollution and environmental degradation.

Keywords: Nanotechnology, green chemistry, photo-catalysis, textile dye, recalcitrant pollutant

1. Introduction

The natural water resources are directly contaminating with pollutants as a result of Industrialization (Attia, Kadhim, and Hussein, 2008; Hill, 2010; Khan, Najeeb and Ishtiaque, 2016). Dyes having synthetic nature show poor biodegradability. Dyeing process releases significant amount of unused dye along with the process water which is harmful to the environment (Wang, 2011). According to the reported estimation around 140,000 tons of synthetic dyes used in dyeing process are released into the environment (Insaf Ayadi, 2016).

Dyes have a profound impact on the aesthetic quality, transparency, and gas solubility of natural water resources. The presence of dyes in water affects the biological activities of aquatic biota (Saxena. and Arputharaj, 2017); (Apostol *et al.*, 2012; Zaharia *et al.*, 2009);(Reyns *et al.*, 2014). The toxicity evaluation studies have reported that dyes have induced toxic as well as mutagenic/ teratogenic impacts on the aquatic biota to name a few breathing impediments, hurdles in swimming, apathy, uncoordinated movements and restlessness, and deformities (Omoregie *et al.*, 1998; Ricking *et al.*, 2014; Srivastava *et al.*, 1995). In water sediments, dyes have also shown strong potential in causing toxicological impacts to aquatic biota (Tkaczyk *et al.*, 2020). Therefore, the interaction of dyes with the sediments; immobilization and dissolution of dyes is highly crucial for determining toxicity effects of the dyes. At different trophic levels the process of adsorption, biotransformation, bioaccumulation in aquatic organisms especially fishes, leads to biomagnification and its impact on humans.

Therefore, it is imperative to degrade or remove these dyes form the waste effluent in efficient manner to avoid such vast impacts.

The degradation of organic pollutants through photocatalytic activity is a well-known fact established by scientific society (Gaya and Abdullah, 2008; Stafford *et al.*, 1996; Umar and Aziz, 2013). It is a type of Advanced Oxidation Process (AOP) that converts recalcitrant colored compounds into colorless reductive metabolites. The presence of a catalyst in this process helps in generating high reactive species (radicals) to enhance the degradation of dyes. Semi-conductors like TiO_2 are very effective catalyst that can degrade pollutants either in mobile (suspended) or immobile (fixed onto suitable substrate) state in aqueous solutions. The effectiveness of TiO_2 as catalyst is attributed to its non- toxic and water insoluble nature, strong oxidation capability, chemical and thermal stability, and has relatively low cost (Feryal Akbal, 2003; Saravanan, 2017; Saravanan, 2013). But in last few years nanotechnology as a multidisciplinary approach has made immense advancements as the improved properties of substances at nanoscale gives wide range of applications in varied fields of sciences. With the intervention of nanotechnology, the properties of a photocatalyst can be enhanced for best performance. In this regard, metallic nanoparticles have shown immense potential to carry out complete mineralization of the recalcitrant organic pollutants (Bharathi *et al.*, 2019; Suellen Aparecida Alves, 2018; Zanella *et al.*, 2018; Zheng *et al.*, 2015). Therefore metallic nanoparticles have huge scope in various aspects of environmental remediation such as, waste water treatment, dye degradation and pollution load reduction (Anupritee Das, 2019; Inam Ullah, 2012).

This study focuses on the synthesis and performance of TiO_2 photocatalyst at nano scale to treat methylene blue dye solution. Green synthesis of TiO_2 nanoparticles is done by using plant extract Fort this study Response Surface Methodology (RSM) has been selected to determine the interactions between the process variables with the least number of experiments. In RSM, a multi-level factorial design: Central Composite Design (CCD) is used that gives minimum experimental runs in comparison to full factorial design (Shah and Tahir, 2020).

2. Materials and method

2.1. Reagents and materials

In the work, analytical grade chemicals were used such as Titanium Tetrachloride ($TiCl_4$) solution (Daejung), Ethanol (Merck), Ammonia (Merck), Methylene Blue (MB) C.I. 52015 dye (Scharlau), NaOH CAS.no. 1310-73-2 (Omicron Sciences Ltd). *Mangifera indica* plant (leaves extract) from the author's institute garden, University of Karachi. Millipore water and distilled water for synthesizing nanoparticle were also used.

2.2. Instrumentation

UV/VIS Spectrophotometer (T80 UV-Visible Spectro-photometer) is used for determining absorbance of methylene blue dye sample solution, Magnetic stirrer (78 HW-1-Serial) for stirring sample solution, Mercury Bulb as UV-C light source (160W, Philips, the Netherland), Portable pH/EC/TDS/Temperature Meter (Hanna-HI9811-5) for determining pH of sample solution, Electronic balance (Meter College 150-Balance) for weighing, Biobase Centrifuge machine (TGL-16 Capacity: 30X28X26CM) to have supernatant solution of sample after treatment to determine final absorbance, FT-IR (Nicolet 67000) within the range of 400 – 4000 cm^{-1} for determining functional groups.

2.3. Experimental Setup and Procedure

The photocatalytic reactor cell was designed as shown in **Figure 1**. A wooden chamber containing UV source bulb clamped on a stand with a still water bath setup placed over the magnetic stirrer. The beaker containing sample solution was placed into the still water bath container to perform experiments.

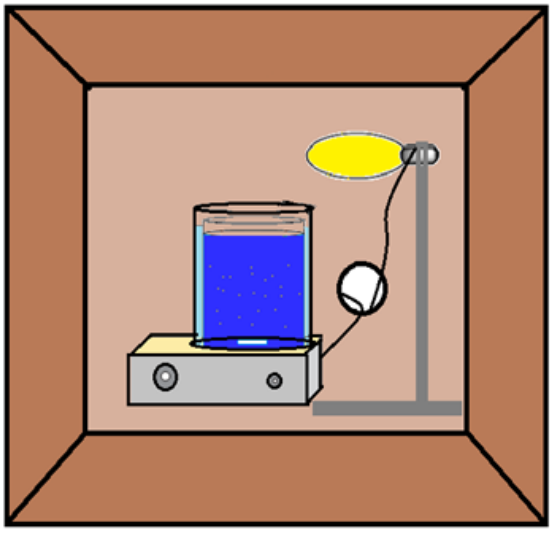

Figure 1. The Experimental Reactor Cell Setup for Photocatalysis Process

For the experimentation, first MB dye solution (250ml) of desired concentration was prepared. The initial absorbance of the sample solution was taken at lambda max value (665 λ) of the dye. HCl and NaOH solutions were used to adjust pH of the solution. Then the quantity of TiO_2 nanoparticle was taken in grams for sample solution. Finally, the beaker with sample solution was placed into the container exposed to the UV source with continuous stirring for predefined duration. After the end of reaction duration, the nanoparticles were removed from the sample solution through centrifuge machine. The final absorbance was taken for the clear sample solution to determine residual dye concentration in the treated sample solution. At the end the percent removal of dye was determined by the following formula.

$$\%\,\text{Removal} = \frac{Ao - At}{Ao} \times 100 \quad (1)$$

Where,

Ao= Initial absorbance of dye solution

At= Final absorbance of dye solution

2.4. Statistical analysis experimental design

Central Composite Design (CCD) is a preferred design for the optimization of operational variables (process parameters) under study to get optimum level of parameters to treat MB dye solution (Hafizi *et al.*, 2013; Shah and Tahir, 2020). The design has been broadly used for process optimization in photocatalytic degradation, adsorption, electrocoagulation, Fenton's oxidation, reduction reactions, biological treatment (Khataee *et al.*, 2011). In RSM, CCD is one of the most commonly used experimental design for developing second-order polynomial model response (Khataee *et al.*, 2011). The second order polynomial model (equation) is given as follows:

$$y = \beta_0 + \sum_{i=1}^{k} \beta_i x_i + \sum_{i=1}^{k} \beta_{ii} x_i^2 + \sum_{i=1}^{k} + \sum_{i \neq j=1}^{k} \beta_{ij} x_i x_j + \varepsilon \qquad (2)$$

Where, Y = is the dependent factor used to predict response of the system, Xij= independent factor, β0= constant coefficient, βi= linear coefficient, βij= interaction coefficient, and βii=quadratic coefficient.

3. Result and discussion

3.1. TiO_2 NPs synthesis and characterization

3.1.1. FTIR analysis

3.1.1.1. FTIR analysis of leaves extract

FTIR spectroscopy was carried out to detect chemical groups present in the leaves extract which in turn indicates the presence of possible biomolecules that are acting as the reducing or capping agent for metallic ion (Ti^{+4}). The FTIR spectrum of *Mangifera indica* leaves extract is shown in Figure 2. Broad band at 3448.72 ≈ 3449 cm^{-1} is due to stretching vibrations of hydroxyl group indicative of alcohols (Rajakumar *et al.*, 2015) and phenols in the leaves extract. The phenolic group is due to the polyphenolic tannins present in plants (EZENAGU, 2008). The small and slightly broad peak at 1384.8 cm^{-1} frequency is for C-O stretch vibrations and H-bonded functional group. Another slightly broad peak appeared at 1643.35 cm^{-1} is indicating C=O stretching of carbonyls and small but sharp peak at 1533.41 cm^{-1} is due to C=C stretching vibrational of alkenes and aromatic rings (Maobe and Nyarango, 2013).

3.1.1.2. FTIR analysis of green TiO_2 nanoparticles

Usually, FTIR spectrum of TiO_2 NPs is recorded in between 4,000 to 500 cm^{-1} absorption bands. Typically, the absorption peaks between 700-400 cm^{-1} frequency is related to Ti-O-Ti bonding (Haider *et al.*, 2015; W. Nachit, 2016) that includes Ti–O stretching and Ti–O–Ti bridging stretching which demonstrates the synthesis of TiO_2 NPs (Goutama, 2018; Yu *et al.*, 2006). The spectrum obtained for newly synthesized TiO_2 NPs is shown in Figure 3. As per the spectrum the absorption peaks recorded at 650, 603, 549, 472 cm^{-1} frequencies indicate the presence of synthesized TiO_2 NPs. A broad peak observed at 3439 cm^{-1} and a small peak at 1643 cm^{-1} are attributed to O-H stretching of hydroxyl group. The presence of hydroxyl group enhances the photocatalytic activity of NPs due to high electron transportability (Wenjuan Li, 2015). Further to it, no peak is appeared at 2900 cm^{-1} for C–H stretching band validating the proper removal of organic compounds because of calcination process (Goutama, 2018).

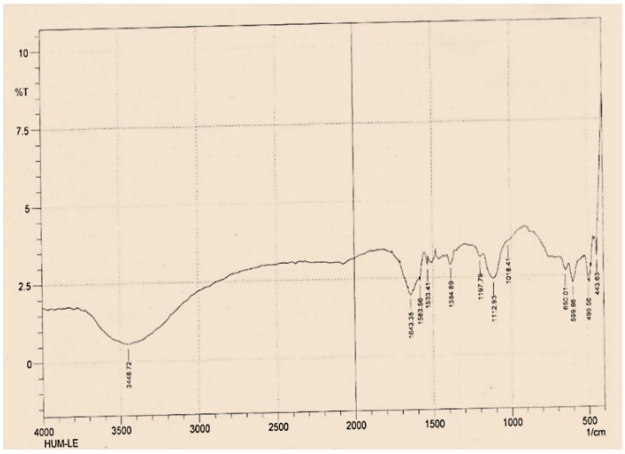

Figure 2. FTIR of Mangifera indica leaves extract

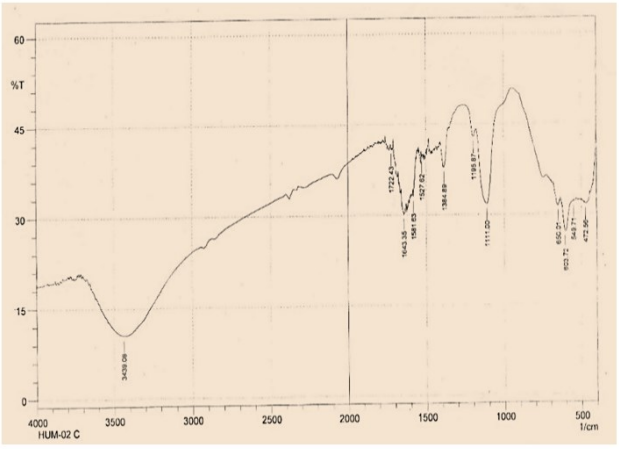

Figure 3. FTIR of Titanium dioxide (TiO_2) Nanoparticle

3.1.2. SEM analysis

The SEM technique is applied to determine the surface morphology of the nanoparticles. According to SEM images shown in Figure 4, the synthesized TiO_2 NPs are present in the form of clusters of irregular shape. The size of the clusters is 200 nm (Nachit, 2016).The basic reason for the irregular morphology is attributed to the possible aggregation of primary particles (Haider *et al.*, 2015). Since, the agglomeration provides more rough and heterogenous surface to the NPs to enhance photocatalytic performance (Goutama, 2018).

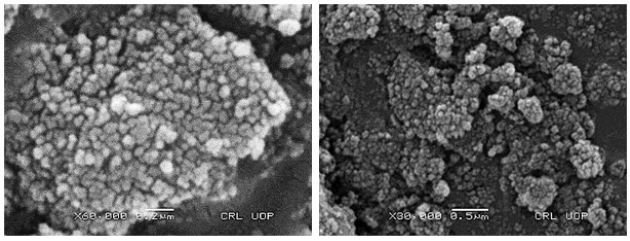

Figure 4. SEM Images of TiO_2 NPs.

3.1.3. EDX/EDS Analysis

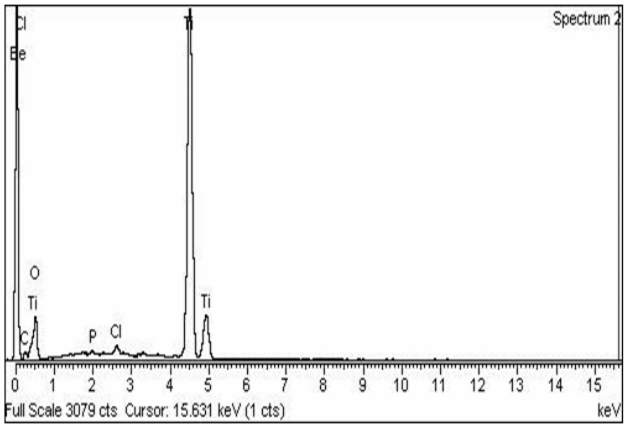

Figure 5. EDX spectra of TiO2 nanoparticles

The elemental composition of the newly synthesized TiO_2 NPs was determined through EDS analysis. Figure 5 shows peaks for elemental Ti and O in the spectra. Besides it, the spectra is also showing peak for C, which is attributed to the use of carbon support film in analysis process. Whereas some minor peaks for other elements like, Cl and P are also observed that are indicative of unknown impurities.

3.1.4. XRD analysis

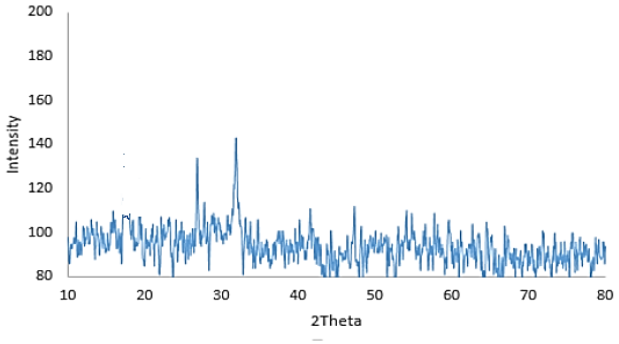

Figure 6. XRD analysis of TiO2 Nanoparticles

The powder XRD pattern of the synthesized TiO_2 NPs by green approach method is shown in Figure 6. It reveals that the TiO_2 NPs are of tetragonal structure and the diffraction peaks detected around 2θ values of 27.32°, 32.79°, 43.18°, 55.18°, and 62.86° with consistent crystal planes of (101), (200), (004), (105) and (204) respectively. This data are well matched with JCPDS card no: 21-1272 (Haider *et al.*, 2017; Jha *et al.*, 2009; Zhao *et al.*, 2007). Additionally, the results suggested that the observed peaks are responsible for anatase phase of TiO_2 NPs.

3.2. Effect of variables on photocatalytic removal of MB dye

3.2.1. Effect of pH

The pH factor was used within the range of 3 to 10. The highest dye removal of 98% was observed for pH value of 4.7. The experimental responses showed that the dye removal performance was improved when pH was 3 to 6.5 at the low dye concentration. However, at the high dye concentration levels it gave low dye removal performance within this range of pH. The surface plots of the dye removal efficiency as a function of pH and dye concentration are shown in Figure 7.

3.2.2. Effect of dye concentration

The factor of dye concentration was studied within the range of 2-10 ppm. The synthetic dye solution with 8 ppm concentration showed maximum dye removal performance of 98 %. Whereas the increased concentration of 10ppm in experimentation showed poor removal performance of 2.39 % . Thus, validating the inverse relationship between the factor such as the dye concentration and its removal efficiency in photocatalysis. The reason anticipated for such decline in the removal performance is because of light emitting photons getting scattered or mirrored due to collisions with the suspended molecules in solution thereby preventing light penetration as a result reduced contact with the catalyst to enhance the removal performance (Shah and Tahir, 2020). This highlights the application of photodegradation process for solutions bearing low color density (Yasmeen, 2019) unless some modification or intervention is made to expedite the removal efficiency. Overall, there was no constant pattern of low removal performance with increasing dye concentration probably due to other factors involved in the process. The surface plot shown in Figure 7 clearly indicates the factor responses.

3.2.3. Effect of amount of nano-photocatalyst

The oxidation rate of the dye is dependent on the generation of strong oxidizing species (hydroxyl radicals) that play the vital role of decolorization in the process of photocatalysis. Therefore, the amount of nano-photocatalyst is crucial for determining process efficiency. The surface plot depicting the removal performance as a function of the amount of nano-photocatalyst and pH is shown in Figure 8. The NPs in the range of 0.04 g - 0.1 g was selected to study factor's response. The highest dye removal efficacy was obtained with 0.04 g of nano-photocatalyst in 8 ppm dye solution. While the minimal efficiency of 19.72 % was noted with the use of 0.1 g of nano-photocatalyst in 6 ppm dye solution. Typically, the removal performance should increase with the increase concentration of nano photocatalyst but the results indicate that efficiency was significantly reduced as the concentration was increased. The reduced performance may be contributed due to scattering of light photons

instead of penetration into the sample solution and interacting with the catalyst. (Shah and Tahir, 2020).

3.2.4. Effect of reaction duration

Typically, the reaction duration is considered important for enhancing the removal performance. Therefore, the greater the time given to the catalyst the higher the chances of converting recalcitrant pollutant into completely mineralized product. However, there are many factors that would not give desired results with increasing reaction time, such as reaction temperature, light intensity, concentration of nano-catalyst and dye etc. The response surface plots of the removal performance as a function of irradiation time and pH and, irradiation time and dye conc. are given as Figures 9 and 10. For this study min to max time duration selected to study factor's response was 30 min - 90 min. It was noted that 45 min of reaction time achieved the maximal removal performance. The optimum duration observed to achieve maximal performance by TiO_2 nano-photocatalyst is halved of the reported time required by the usual TiO_2 catalyst i.e., 90 mint (Shah and Tahir, 2020). This validates the benefits that can be obtained due to enhanced performance at nano scale by the catalyst. Other reaction time at which good performance was noted is 60 min with 95.34% removal performance. However, the maximal process performance observed at 45 min was reduced by 26% at 90 min reaction duration.

Table 1. Model Summary for Methylene Blue Dye Removal

Statistical Variable	Photocatalysis
S (root mean square error)	6.23814
R^2	79.37%
R^2 (adj.)	61.32%

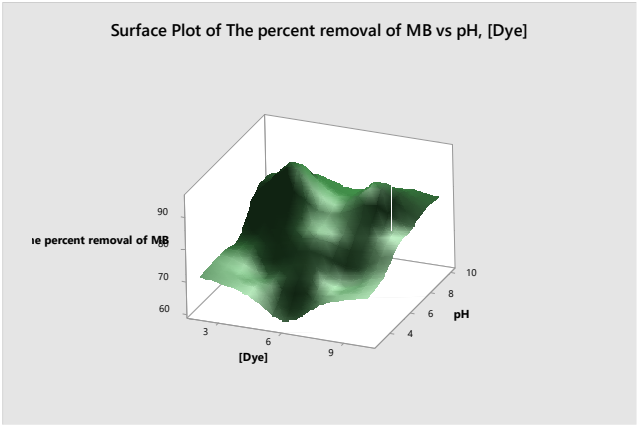

Figure 7. MB dye removal efficiency as a function of pH and dye concentration.

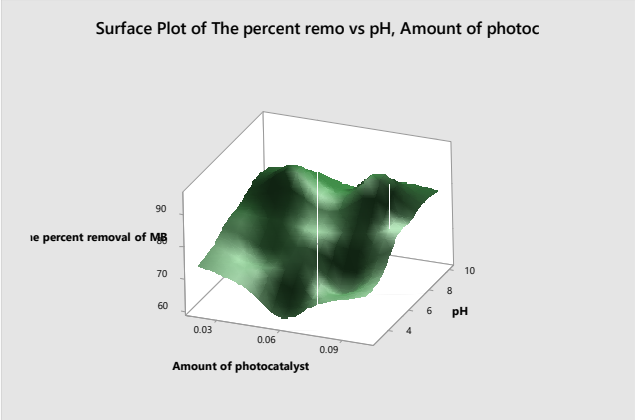

Figure 8. MB dye removal efficiency as a function of pH and amount of nano-photocatalyst.

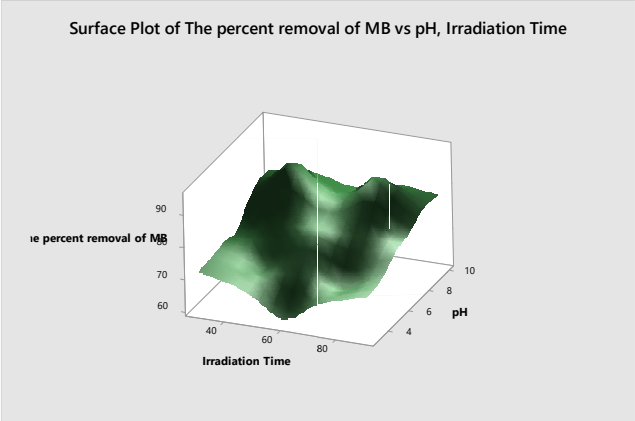

Figure 9. MB dye removal efficiency as a function of Irradiation Time and pH.

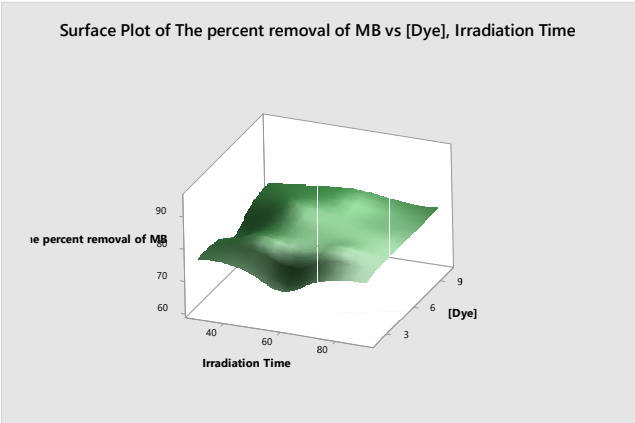

Figure 10. MB dye removal efficiency as a function of Irradiation Time and Dye Concentration.

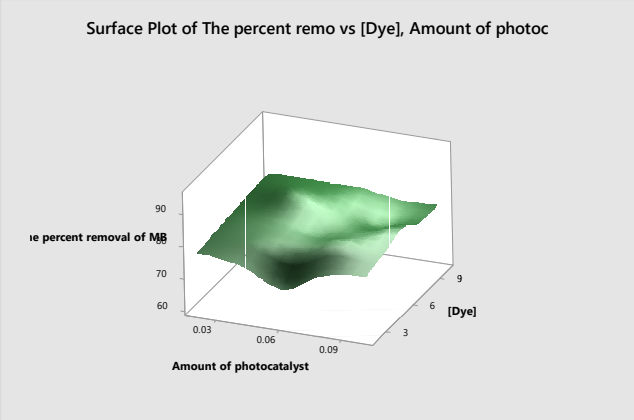

Figure 11. Response surface plots of dye removal performance as a function of nano–photocatalysis and dye concentration

4. Statistical design response

4.1. Determination of coefficients and the residuals analysis

The quantitative evaluation of coefficient of determination (R^2) was made to have a comparison between R^2 and R^2 adjusted values: determining the impact of selected parameters on the process efficiency. The output given by using response surface quadratic model is shown in Table 1. The values of coefficient R^2 and R^2 adjusted in percent were about 79.37% and 61.32% respectively, which deduce that the model is best fitted and acceptable. Further to it, the competency of the model was determined through residual plots. The graph of residual values for expected and observed values is given as Figure 12. It is observed in the normal probability graph that the experimental data values almost have a linear trend as most of the values overlay the true line. Next to it, in the graph of residual versus fits (between residual and fitted data values) for dye removal effectiveness, a scattered pattern has been formed nearby the zero line. The graph of histogram in which randomly fluctuating pattern is visible, and similar pattern is observed in residuals versus the corresponding order of observations graph along the zero-error line.

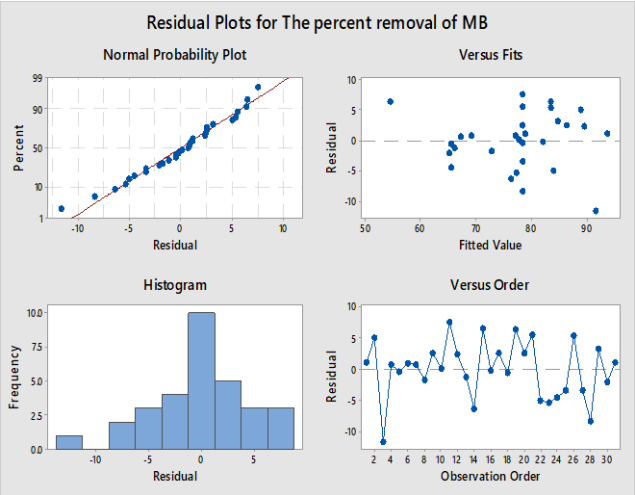

Figure 12. Residual plots for the photodegradation of MB dye using TiO_2 nano-catalyst.

Table 2. ANOVA Analysis during Photocatalysis Process

Source	DF	Adj SS	Adj MS	F Value	P-Value
Regression Model	4	2395.37	171.10	4.40	0.003
Linear	4	2086.83	521.71	13.41	0.000
Square	4	102.16	25.54	0.66	0.631
2-Way Interaction	6	206.38	34.40	0.88	0.529
Error	16	622.63	38.91	*	*
Lack-of-Fit	10	432.92	43.29	1.37	0.364
Pure Error	6	189.71	31.62	*	*
Total	30	3018.00	*	*	*

Table 3. The estimated parameters, t and p-values for MB dye decolorization in photocatalysis Process

Term	Effect	Coef	SE Coef	T-Value	P-Value
Constant		78.43	2.36	33.26	0.000
pH (A)	37.17	18.58	2.55	7.300	0.000
[Dye](B)	2.500	1.250	2.55	0.490	0.630
Amount of TiO_2 (C)	-1.830	-0.920	2.55	-0.360	0.724
Irradation Time(D)	0.500	0.250	2.55	0.100	0.923
pH*pH (A^2)	-10.61	-5.300	4.67	-1.140	0.272
[Dye]*[Dye](B^2)	-1.610	-0.800	4.67	-0.170	0.865
Amount of TiO_2*Amount of TiO_2(C^2)	9.390	4.700	4.67	1.010	0.329
Irradation Time*Irradation Time (D^2)	-1.610	-0.800	4.67	-0.170	0.865
pH*[Dye] (A*B)	-7.500	-3.750	6.24	-0.60	0.556
pH*Amount of TiO_2(A*C)	14.50	7.250	6.24	1.16	0.262
pH*Irradation Time (A*D)	2.500	1.250	6.24	0.20	0.844
[Dye]*Amount of TiO_2 (B*C)	-20.50	-10.25	6.24	-1.64	0.120
[Dye]*Irradation Time (B*D)	-6.500	-3.250	6.24	-0.52	0.610
Amount of TiO_2*Irradation Time(C*D)	9.500	4.750	6.24	0.76	0.457

4.2. Analysis of variance (ANOVA)

In this study the fitness of the model was also determined with the basic statistical tool i.e., ANOVA. While the significance of the model is determined by the help of F-test and Lack of Fit (LOF) test values. The ANOVA estimated at nanoscale is given in Table 2. The P-value estimation on statistical basis determines the significance of the coefficients under study. The p-value estimation for LOF remained above 0.05 resulting into insignificant LOF thereby accepting the model. The determination of student's t and p- test values are also crucial to study the mutual interactions between selected factors/variables. The tested parameters along with t and p- test values are represented in Table 3. If the t-test values are higher and out of these only < 5% values are at significant level, then it is concluded that the corresponding coefficients are important.

5. Conclusion

Green chemistry is a convenient, environmental-friendly, and less harmful approach for synthesizing nanoparticles through means or material of organic origin (biological). The study has shown that the plant leaves extract is a good reducing/capping agent for nanoparticle synthesis. The treatment of methylene blue organic pollutant using green based synthesized nanoparticles of the photocatalyst, enhances the efficiency of the photocatalysis process. In this study the photocatalysis process has shown promising results as a function of dye removal from the system. The application of nanoparticles based on green chemistry in the photocatalytic process can be a sustainable approach to cope with the issues of water pollution and environmental degradation.

Acknowledgment

The authors acknowledge the research grant awarded by Dean Science, University of Karachi for experimental work only in this study and have no conflict of interest.

References

Alves S.A., Goulart L.A., Mascaro L.H. (2018). A novel WO 3/MoS2 photocatalyst applied to the decolorization of the textile dye Reactive Blue 198. *Journal of Solid State Electrochemistry,* **22**(1449–1458). doi:10.1007/s10008-017-3771-4

Apostol L.C., Pereira L., Pereira R., Gavrilescu M., and Alves M.M. (2012). Biological decolorization of xanthene dyes by anaerobic granular biomass. *Biodegradation,* **23**(5), 725–737.

Attia A.J., Kadhim S.H., and Hussein F.H. (2008). Photocatalytic degradation of textile dyeing wastewater using titanium dioxide and zinc oxide. *Journal of Chemistry,* **5**(2), 219–223.

Ayadi I., Souissi Y., Jlassi I., Peixoto F. and Mnif W. (2016). Chemical Synonyms, Molecular Structure and Toxicological Risk Assessment of Synthetic Textile Dyes: A Critical Review. *Journal of Developing Drugs,* **5**(1).

Bharathi P., Harish S., Archana J., Navaneethan M., Ponnusamy S., Muthamizhchelvan C. and Hayakawa Y. (2019). Enhanced charge transfer and separation of hierarchical CuO/ZnO composites: The synergistic effect of photocatalysis for the mineralization of organic pollutant in water. *Applied Surface Science,* **484**, 884–891.

Das A., Madhu K., Bharti A., Kumar P. (2019). Nanotechnology and it's applications in environmental remediation: an overview. *International Journal of Plant Research,* **11**. doi:https://doi.org/10.1007/s42535-019-00040-5

Feryal Akbal A.N.O. (2003). Photocatalytic Degradation Of Phenol. *Environmental Monitoring and Assessment,* **83**, 295–302.

Gaya U.I., and Abdullah A.H. (2008). Heterogeneous photocatalytic degradation of organic contaminants over titanium dioxide: a review of fundamentals, progress and problems. *Journal of photochemistry and photobiology C: Photochemistry reviews,* **9**(1), 1–12.

Goutama S.P., Saxena G., Singh V., Yadav A.K., Bharagava R.N., Thapa K.B. (2018). Green synthesis of TiO2 nanoparticles using leaf extract of Jatropha curcas L. for photocatalytic degradation of tannery wastewater. *Chemical Engineering Journal,* **336**, 386–396. doi:https://doi.org/10.1016/j.cej.2017.12.029

Hafizi A., Ahmadpour A., Koolivand-Salooki M., Heravi M., and Bamoharram F. (2013). Comparison of RSM and ANN for the investigation of linear alkylbenzene synthesis over H14 [NaP5W30O110]/SiO2 catalyst. *Journal of Industrial and Engineering Chemistry,* **19**(6), 1981–1989.

Haider A.J., AL- Anbari R.H., Kadhimb G.R., and Salame C.T. (2017). Exploring potential Environmental applications of TiO2 Nanoparticles *Energy Procedia,* **119**, 332–345.

Haider A.J., Jameel Z.N., and Taha S.Y. (2015). Synthesis and Characterization of TiO2 Nanoparticles via Sol-Gel Method by Pulse Laser Ablation *Engineering And Technology Journal,* **33**(5).

Hill M.K. (2010). *Understanding Environmental Pollution* (Third ed.): Cambridge University Press.

Inam Ullah S. A., Hanif M.A. and Shahi S.A. (2012). Nanoscience for environmental remediation: A Review. *International Journal of Chemical and Biochemical Sciences,* **2** 60–77.

Jha A.K., Prasad K., and Kulkarni A. (2009). Synthesis of TiO2 nanoparticles using microorganisms. *Colloids and Surfaces B: Biointerfaces,* **71**(2), 226–229.

Khan W., Najeeb I., and Ishtiaque S. (2016). Photocatalytic degradation of a real textile wastewater using titanium dioxide, zinc oxide and hydrogen peroxide. *International Journal of Engineering Science,* **5**(7), 61–70.

Khataee A.R., Kasiri M.B. and Alidokht L. (2011). Application of response surface methodology in the optimization of photocatalytic removal of environmental pollutants using nanocatalysts. *Environmental technology,* **32**(15), 1669–1684. doi:10.1080/09593330.2011.597432

Li W., Yan T., Kong D., You J. and Li D. (2015). Relationship between surface hydroxyl groups and liquid-phase photocatalytic activity of titanium dioxide. *Journal of Colloid and Interface Science,* **444**, 42–48. doi: https://doi.org/10.1016/j.jcis.2014.12.052

Maobe M.A. and Nyarango R.M. (2013). Fourier Transformer Infra-Red Spectrophotometer Analysis of Warburgia ugandensis Medicinal Herb Used for the Treatment of Diabetes, Malaria and Pneumonia in Kisii Region, Southwest Kenya. *Global Journal of Pharmacology,* **7**(1), 61–68. doi:10.5829/idosi.gjp.2013.7.1.7226

Nachit W., Touhtouh S., Ramzi Z., Zbair M., Eddiai A., Rguiti M., Bouchikhi A., Hajjaji A. and Benkhouja K. (2016). Synthesis of nanosized TiO2 powder by sol gel method at low temperature. *Molecular Crystals and Liquid Crystals,* **627**, 170–175. doi:10.1080/15421406.2015.1137135

Okwu D.E. and Ezenagu V.I.T.U.S. (2008). Evaluation Of The phytochemical composition of mango (Mangifera indica Linn) stem bark and leaves *International Journal of Chemical Sciences,* **6**(2), 705–716.

Omoregie E., Ofojekwu P., Anosike J., and Adeleye A. (1998). Acute toxicity of malachite green to the Nile tilapia, Oreochromis niloticus (L.). *Journal of Aquaculture in the Tropics,* **13**(4), 233–237.

Rajakumar G., Rahuman A.A., Roopan S.M., Chung I.M., Anbarasan K., and Karthikeyan V. (2015). Efficacy of larvicidal activity of green synthesized titanium dioxide nanoparticles using Mangifera indica extract against blood-feeding parasites. *Parasitology Research,* **114**(2), 571–581. doi:10.1007/s00436-014-4219-8

Reyns T., Belpaire C., Geeraerts C., and Van Loco J. (2014). Multi-dye residue analysis of triarylmethane, xanthene, phenothiazine and phenoxazine dyes in fish tissues by ultra-performance liquid chromatography–tandem mass spectrometry. *Journal of Chromatography B,* **953**, 92–101.

Ricking M., Schwarzbauer J. and Petra A. (2014). Malachite green in suspended particulate matter and surface sediments in Germany. Report. Federal Environment Agency, Berlin, Germany. In.

Saravanan R., Gracia F. and. Stephen A. (2017). Basic Principles, Mechanism, and Challenges of Photocatalysis. In.

Saravanan R., Gupta V.K., Narayanan V., Arumainathan S. (2013). Comparative study on photocatalytic activity of ZnO prepared by different methods. *Journal of Molecular Liquids,* **181**, 133–141. doi: 10.1016/j.molliq.2013.02.023

Saxena S., Raja A.S.M. and Arputharaj A. (2017). Challenges in Sustainable Wet Processing of Textiles. *Textile Science and Clothing Technology*, 43–79.

Shah A.R., and Tahir H. (2020). The photodegradation of tri-dyes in the real textile effluent of SITE industrial zone of Karachi city based on central composite design. *Indian Chemical Engineer*, 1–15.

Srivastava S., Singh N., Srivastava A.K. and Sinha R. (1995). Acute toxicity of malachite green and its effects on certain blood parameters of a catfish, Heteropneustes fossilis. *Aquatic toxicology,* **31**(3), 241–247.

Stafford U., Gray K.A. and Kamat P.V. (1996). Photocatalytic degradation of organic contaminants: Halophenols and related model compounds. *Heterogeneous Chemistry Reviews,* **3**(2), 77–104.

Tkaczyk A., Mitrowska K., and Posyniak A. (2020). Synthetic organic dyes as contaminants of the aquatic environment and their implications for ecosystems: a review. *Science of The Total Environment,* **717**, 137222.

Umar M., and Aziz H.A. (2013). Photocatalytic degradation of organic pollutants in water. *Organic pollutants-monitoring, risk and treatment,* **8**, 196–197.

Wang Z., Xue M., Huang K. and Liu Z. (2011). Textile Dyeing Wastewater Treatment. In P. J. Hauser (Ed.), *Advances in Treating Textile Effluent* (**162**). China: InTech.

Yasmeen T. (2019). *The application of Nanotechnology; Electrochemistry for the removal of organic and Inorganic Pollutants.* (M.Phil), University of Karachi, Karachi.

Yu J., Su Y., Cheng B. and Zhou M. (2006). Effects of pH on the microstructures and photocatalytic activity of mesoporous nanocrystalline titania powders prepared via hydrothermal method. *Journal of Molecular Catalysis A: Chemical,* **258**(1–2), 104–112. doi:10.1016/j.molcata.2006.05.036

Zaharia C., Suteu D., Muresan A., Muresan R. and Popescu A. (2009). Textile wastewater treatment by homogenous oxidation with hydrogen peroxide. *Environmental Engineering and Management Journal,* **8**(6), 1359–1369.

Zanella R., Avella E., Ramírez-Zamora R.M., Castillón-Barraza F. and Durán-Álvarez J.C. (2018). Enhanced photocatalytic degradation of sulfamethoxazole by deposition of Au, Ag and Cu metallic nanoparticles on TiO2. *Environmental technology,* **39**(18), 2353–2364.

Zhao Y., Li C., Liu X., Gu F., Jiang H., Shao W. and He Y. (2007). Synthesis and optical properties of TiO2 nanoparticles. *Materials Letters,* **61**(1), 79–83.

Zheng X., Li D., Li X., Chen J., Cao C., Fang J. and Zheng Y. (2015). Construction of ZnO/TiO2 photonic crystal heterostructures for enhanced photocatalytic properties. *Applied Catalysis B: Environmental,* **168**, 408–415.